J Mater Sci: Mater Electron (2016) 27:10347–10352
DOI 10.1007/s10854-016-5120-2

Rheological phase reaction synthesis of Co-doped $LiMn_2O_4$ octahedral particles

Zonghui Yi[1,2]

Received: 24 March 2016 / Accepted: 2 June 2016 / Published online: 15 June 2016

Abstract Co-doped $LiMn_2O_4$ octahedral particles were prepared by the rheological phase reaction using $LiOH{\cdot}H_2O$, electrolytic manganese dioxide (EMD), and Co_3O_4 as starting materials. The crystal structure and morphology of as-synthesized compound were characterized by X-ray diffraction (XRD) and scanning electron microscopy (SEM). The XRD results showed that the obtained powders were single-phase with a cubic spinel structure (Fd3m space group). SEM micrograph revealed that the particles possessed an octahedral morphology, with an average particle size of about 1–2 μm. Electrochemical test results showed that this Co-doped $LiMn_2O_4$ could deliver high specific capacity and good cycling stability, for the initial discharge capacity was 112.5 mAh g^{-1} and the discharge capacity remained to keep 100 mAh g^{-1} at 100th cycle, with an average capacity fade rate about 0.1 % per cycle.

1 Introduction

The exhaustion of natural resources and environmental concerns of greenhouse gas emissions have stimulated the significant development of lithium ion batteries for large energy storage applications, like plug-in hybrid electric vehicles (PHEVs) and electric vehicles (EVs) [1]. However, commercialization of these batteries promotes the further exploitation of inexpensive cathode candidates with superior electrochemical performance. $LiMn_2O_4$ is considered as one of the most promising cathode materials for potential application in the PHEVs and EVs. Compared to Co or Ni based cathode materials, $LiMn_2O_4$ has many attractive features, like low cost, low toxicity, abundant resources, high charge/discharge voltage and increased safety margin to over-charge conditions [2].

But the severe capacity fade upon cycling, which is mainly due to the structural instability caused usually by Mn^{3+} disproportionation reaction and Jahn–Teller distortion, hinders the development of the spinel cathode material. Introducing partial alien cation in the Mn sites (octahedral 16d sites) in the lattice of spinel is considered as one of the most effective strategies to improve cycling performance of $LiMn_2O_4$ electrode. Recently, researchers have extensively studied the structure and property of M-doped $LiMn_2O_4$ cathode materials (M = Ti, Fe, Co, Zn, Al, Mg, Cr, Ni, Cu, etc.) [3–8]. Among these dopants, Co has been expected to be the most effective dopant. It was reported that Co-doped $LiMn_2O_4$ spinel exhibited enhanced electrochemical performance, compared to undoped $LiMn_2O_4$ [9].

Conventionally, commercial $LiMn_2O_4$ is widely prepared by solid-state reaction, which requires high sintering temperature and prolonged sintering time. Other alternative methods have been explored to overcome these shortcomings [10–14]. However, most of them contain multi-step and time-consuming processes, which undoubtedly increases the production cost of the spinel cathode material.

In this study, Co-doped $LiMn_2O_4$ octahedral particles were synthesized via a simple rheological phase reaction which does not need troublesome processes such as palletizing, washing, stirring and repeated heat treatment [15].

✉ Zonghui Yi
yzonghui@yeah.net

[1] College of Chemistry and Chemical Engineering, Ningxia Normal University, Guyuan 756000, China

[2] Engineering and Technology Research Center of Liupanshan Resources, Ningxia Normal University, Guyuan 756000, China

Co would substitute for partial Mn to improve the cycling performance. The effects of rheological phase reaction and Co doping on the structure, morphology and electrochemical performance of the spinel material were investigated in detail.

2 Experimental

All the reagents were purchased from commercial sources and used without further purification. Co-doped $LiMn_2O_4$ cathode material was synthesized by the rheological phase reaction method. $LiOH{\cdot}H_2O$, EMD, and Co_3O_4 were used as starting materials. The starting materials were mixed by grinding at a nominal atomic ratio of 1.03: 1.95: 0.05 respectively for Li: Mn: Co, with an approximate formula $LiMn_{1.95}Co_{0.05}O_4$. A proper amount of de-ionized water was added to get a rheological body and the mixture was heated at 100 °C for 5 h in a Teflon-lined stainless autoclave. After dried at 120 °C, the precursor was moved into quartz tube and heated in air atmosphere at a rate of 10 °C min^{-1} from room temperature to 800 °C, held at 800 °C for 10 h, naturally cooled to room temperature, the Co-doped $LiMn_2O_4$ material was obtained. All the procedures are summarized in Fig. 1. For comparison, $LiMn_2O_4$ was also synthesized by the same method.

The X-ray diffraction (XRD) measurement was carried out with a Bruker D8 Advance X-ray diffractometer (Germany) with Cu Kα radiation (λ = 1.54056 Å). Data was collected between 10° and 80° with a scan speed of 4° min^{-1}. The particle size and morphological features were revealed by scanning electron microscope (SEM, JEOL JSM-6700F, Japan).

The galvanostatic charge/discharge tests were carried out using the coin-type cell (size: 2016), which used as-prepared spinel materials as the working electrode and a lithium foil as the counter electrode. Working electrode was fabricated by mixing 85 wt% spinel powder with 8 wt% acetylene black and 7 wt% PVDF binder, coating the mixture onto an aluminum foil current collector. The electrolyte was the solution of 1 mol L^{-1} $LiPF_6$ dissolved in EC/DMC (1:1 volume ratio). A porous polypropylene film (Celgard 2300) was used to separate two electrodes. The cells were assembled in an argon-filled Unilab-2000 glove box (Mbraun, Germany). The cells were charged and discharged between 3.2 and 4.25 V versus Li/Li^+ at a constant current density of 30 mA g^{-1}. All the electrochemical measurements of the cells were performed at room temperature on a Neware battery test system (Newell, China).

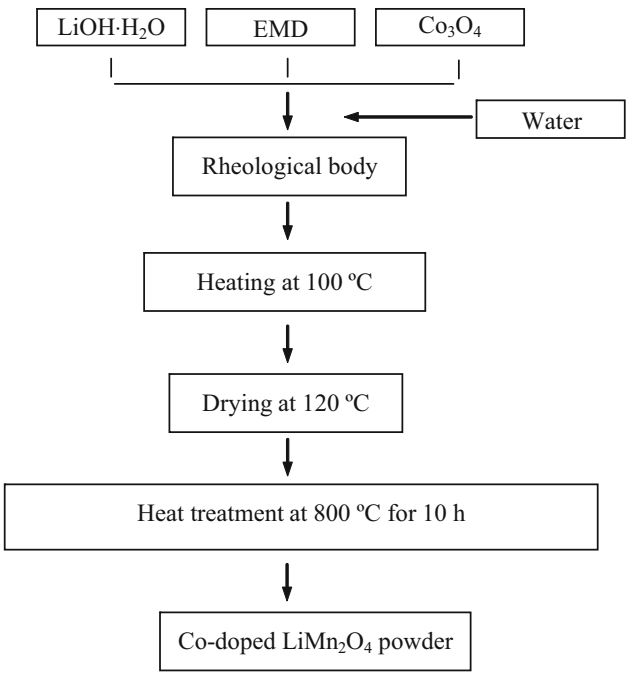

Fig. 1 Process flow chart of Co-doped $LiMn_2O_4$

3 Results and discussion

3.1 Structural analysis

Co-doped $LiMn_2O_4$ was reported to crystallize in the normal spinel structure with a general formula $A[B_2]O_4$ [9]. Figure 2 shows the crystal structure of Co-doped $LiMn_2O_4$, in this spinel structure, A (Li^+ ions) occupy the tetrahedral Wyckoff 8a sites and B (Mn^{3+}, Co^{3+} and Mn^{4+} ions) occupy the octahedral 16d sites, while O^{2-} ions are located in 32e sites. XRD pattern of as-synthesized Co-doped $LiMn_2O_4$ is presented in Fig. 3. The sharp and strong diffraction peaks indicate that the sample is well crystallized. No impurity phases are detected in the sample. All diffraction peaks of the sample can be perfectly indexed as the cubic spinel with the Fd3m space group (JCPDS no. 35–0782). No clear (220) peak (at ca. $2\theta = 30.6°$) is observed in the XRD pattern, indicating the low degree of the cation mixing for the Co-doped $LiMn_2O_4$. The intensity ratio of the (400)/(311) peaks in the XRD pattern is high, also indicating the low degree of the cation mixing. The low degree of the cation mixing suggests that migration of Li^+ ions through the three-dimensional tunnels in Co-doped $LiMn_2O_4$ is significantly facilitated due to less M (M = Mn and/or Co) ions in Li^+ sites as hindrance. Thus, the three-dimensional framework of Co-doped $LiMn_2O_4$ is well constructed by $Mn_{0.975}Co_{0.025}O_6$ octahedra and LiO_4 tetrahedra. The crystal lattice parameter of Co-doped $LiMn_2O_4$, calculated by means of least-square method in terms of cubic space group, is 8.211 by Rietveld analysis,

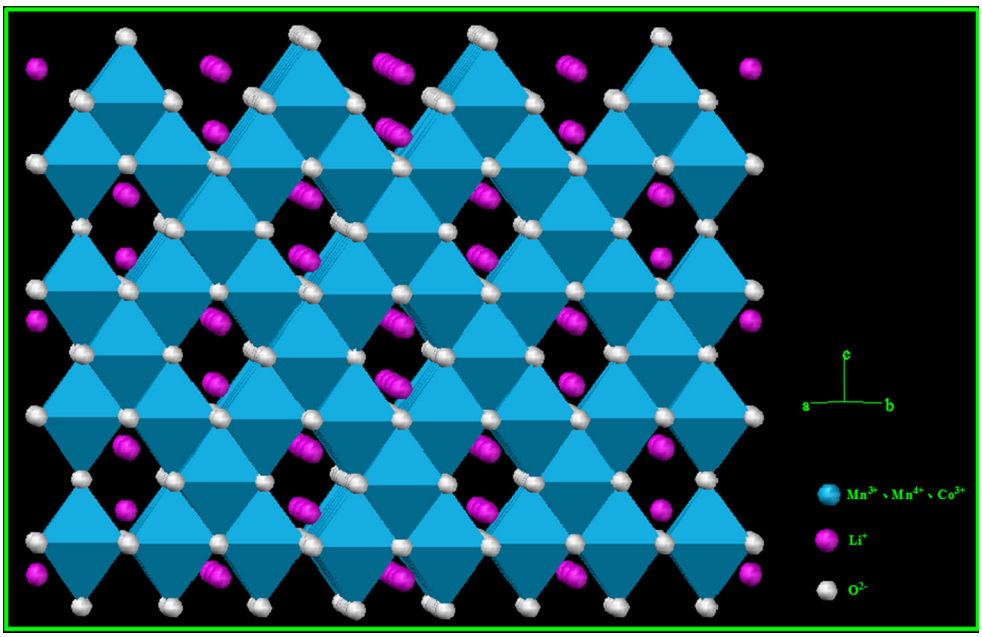

Fig. 2 Crystal structure of Co-doped $LiMn_2O_4$

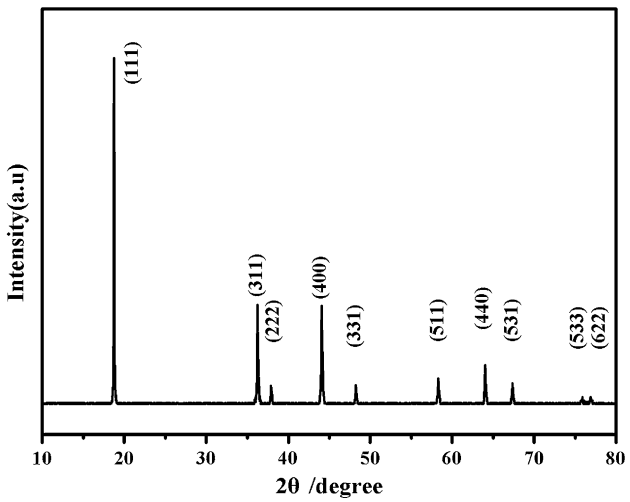

Fig. 3 XRD pattern of Co-doped $LiMn_2O_4$

smaller than that of un-doped $LiMn_2O_4$ from a standard database (8.248).

The radius of Co^{3+} ion (0.63 Å) is smaller than that of Mn^{3+} ion (0.66 Å) and the bond energy of Co^{3+}–O (1067 kJ mol^{-1}) in the MO_6 octahedra is higher than that of Mn^{3+}–O (946 kJ mol^{-1}). The unit cell volume is assumed to shrink when Co^{3+} ions substitute for partial Mn^{3+} ions in the octahedral 16d sites. The result of XRD analysis presented above is consistent with the assumption. The smaller and more stable Co^{3+} (no Jahn–Teller effect) ion and the stronger Co^{3+}–O bond suggest the enhanced stability of $Mn_{0.975}Co_{0.025}O_6$ octahedra at deeply discharged state. Moreover, the decreased Mn^{3+} content in Co-doped $LiMn_2O_4$, compared to that in un-doped $LiMn_2O_4$, is expected to effectively restrain the Jahn–Teller effect of $Mn_{0.975}Co_{0.025}O_6$ octahedra and simultaneously suppress the occurrence of Mn dissolution during electrochemical cycling.

Apparently, well-ordered cubic spinel structure has been formed via the facile rheological phase reaction. High crystallinity might be associated with the rheological phase reaction. During the rheological phase treatment, all reactants could be homogeneously mixed; the surface area of the solid particles could be utilized efficiently; and the contact between solid particles and fluid could be wide and close. Thus Li^+ ions in the rheological body could easily diffuse to the surface and the tunnels (1 × 1 tunnel and 1 × 2 tunnel) which exist in EMD crystal, resulting in a homogeneous mixing of reactants even at atomic scale, as shown in Fig. 4. The diffusion distance of Li, Mn and/or Co cations required for the construction of spinel lattice would thus be shortened, which could promote the crystallization process.

3.2 Morphology analysis

Morphology control is essential to the electrochemical performance of Mn-based spinel cathode. Figure 5 presents the SEM image of Co-doped $LiMn_2O_4$. Apparently, the sample comprises of submicron single-crystalline particles. These particles have a perfect octahedral morphology with obvious sharp edges between the facets. The particle surface is rather smooth. The average particle size from SEM image is around 1–2 μm with a narrow particle size distribution. It is well known that the uniform particle size distribution leads to the uniform depth of charge/discharge

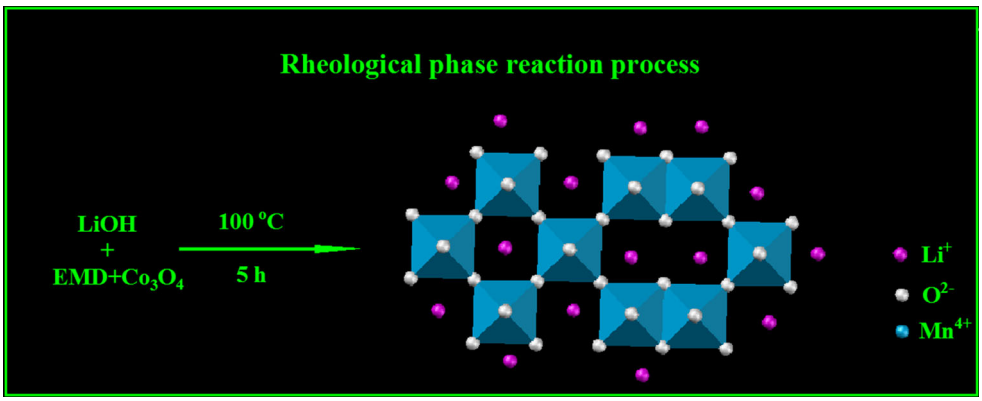

Fig. 4 Schematic illustration of the mixing of the starting materials

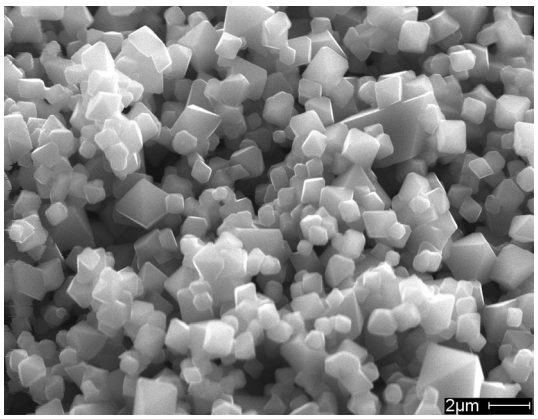

Fig. 5 SEM image of Co-doped $LiMn_2O_4$

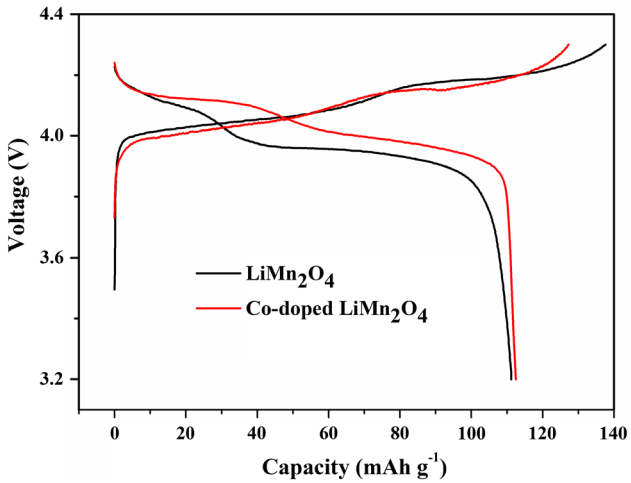

Fig. 6 The first discharge–charge curves of Co-doped $LiMn_2O_4$ and $LiMn_2O_4$ at a current density of 30 mA g^{-1} between 3.2 and 4.25 V

(DOC/DOD) of each particle, which favors to increase the utilization of the material to enhance the global battery performance, which also favors to enhance the global structural stability by alleviating the accumulation of Li^+ or Mn^{4+} ions on some fine particles during electrochemical cycling.

3.3 Electrochemical performance

The electrochemical performance of Mn-based spinel material is influenced by its crystallographic structure, chemical composition, morphological characteristics, particle size and particle size distribution. Figure 6 shows the initial charge–discharge curve of Co-doped $LiMn_2O_4$ at a moderate current density of 30 mA g^{-1} between 3.2 and 4.25 V. Similar to typical charge–discharge curve of $LiMn_2O_4$ reported previously [16], the initial charge–discharge curve of Co-doped $LiMn_2O_4$ shows two obvious voltage plateaus, indicating the mechanism for Li^+ ions extracting from/inserting into this sample is similar to that for Li^+ ions extracting from/inserting into typical $LiMn_2O_4$: plateaus at approximately 4.0/3.95 V range correspond to the extraction/insertion of Li^+ ions from/into one half of the tetrahedral sites with Li–Li interaction, while those at 4.15/4.10 V range correspond to the extraction/insertion of Li^+ ions from/into the other half of the tetrahedral sites without Li–Li interaction.

The initial charge capacity of Co-doped $LiMn_2O_4$ is 127.3 mAh g^{-1}. The initial discharge capacity of Co-doped $LiMn_2O_4$ is 112.5 mAh g^{-1}, and the initial coulombic efficiency is 88.4 %. The initial irreversible capacity of Co-doped $LiMn_2O_4$ is 14.8 mAh g^{-1}, which mainly results from oxidation decomposition of electrolyte occurring mainly on the surface of the cathode material at high potentials in the charge process. While $LiMn_2O_4$ electrode delivers the initial charge/discharge capacity of 137.7 and 111.2 mAh g^{-1}, respectively. This result suggests that Co-doped $LiMn_2O_4$ shows higher electrochemical activity and better reversibility than un-doped $LiMn_2O_4$.

Figure 7 shows the cycling performances of the Co-doped $LiMn_2O_4$ and $LiMn_2O_4$ at a current density of 30 mA g^{-1} between 3.2 and 4.25 V at room temperature. As seen from Fig. 7, $LiMn_2O_4$ displays poor capacity

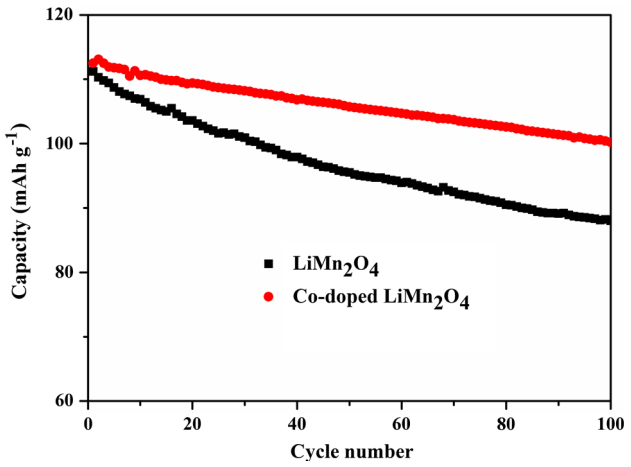

Fig. 7 Cycling performances of Co-doped $LiMn_2O_4$ and $LiMn_2O_4$ at a current density of 30 mA g^{-1} between 3.2 and 4.25 V

retention. The discharge capacity of $LiMn_2O_4$ fades from 111.2 to 87.9 mAh g^{-1} at 100th cycle, with the capacity retention of 79 %. While Co-doped $LiMn_2O_4$ electrode displays much better cycling performance. The discharge capacity of this Co-doped $LiMn_2O_4$ remains to keep 100 mAh g^{-1} at 100th cycle. The discharge capacity retention from the first to the 100th cycle is around 88.9 %, with an average capacity fade rate around 0.1 % per cycle. The efficiency of the Li^+ insertion/deinsertion processes for the Co-doped $LiMn_2O_4$ gradually increases and reaches 99 % after 2 cycles.

As is known, the rapid capacity fade of spinel $LiMn_2O_4$ is caused mainly by its structural instability associated usually with two factors. The e-orbital degeneracy on a localized Mn^{3+} in sufficient concentration gives rise to a cooperative orbital ordering to lower the Mn^{3+} site symmetry from O_h to O_t. This phenomenon is referred to a Jahn–Teller distortion. In the deeply discharged spinel $LiMn_2O_4$ electrode under nonequilibrium conditions, accumulation of Li^+ renders Li^+ to intercalate into octahedral 16c site to form a $Li_2Mn_2O_4$ cubic spinel phase with high Mn^{3+} ion concentration, which immediately relaxes to a tetragonal spinel phase ($[Li]_2^{8d}[Mn]_2^{8c}O_4$, I41/amd) accompanied by a large unit cell expansion. Besides, on the surface of spinel $LiMn_2O_4$ particles at deeply discharged state, accumulation of Li^+ gives a high enough concentration of Mn^{3+} on the surface for the disproportionation reaction $2Mn^{3+} \rightarrow Mn^{2+} + Mn^{4+}$, which leads to a dissolution of Mn^{2+} into the electrolyte.

The partial substitution of Co^{3+} ions for Mn^{3+} ions in the $[Mn_2]O_4$ framework lowers the occurrence of Li^+ accumulation at deeply discharged state, which lowers the Mn^{3+} concentration consequently to alleviate Jahn–Teller distortion and Mn^{3+} disproportionation reaction. Besides, since the radius of Co^{3+} is smaller than that of Mn^{3+} and bond energy of Co^{3+}–O is bigger than that of Mn^{3+}–O, Co doping can enhance the overall $Mn_{1-x}Co_xO_6$ ($0 < x < 1$) framework in deeply discharged electrode. This is also thought to efficiently suppress Jahn–Teller distortion and prevent manganese from dissolving into electrolyte to some extent.

On the other hand, the high crystallinity and low degree of the cation mixing, which probably benefited from the rheological phase reaction that ensures atomic scale-mixing of Li, Mn and Co constituents, are also greatly beneficial for improving the electrochemical performance of the Co-doped $LiMn_2O_4$ material.

Moreover, such superior cycling performance of octahedral Co-doped $LiMn_2O_4$ may also be attributed to its unique octahedral shape. It was reported that Mn dissolution largely relied on the crystalline orientation of the surface exposed to the electrolyte. Kim et al. found that truncated octahedron $LiMn_2O_4$ with exposed {111} surface was more resistant against the Mn dissolution in comparison with nanoplatelets with {110} surface [17]. Also, Jin et al. [18] considered that the octahedral morphology was the very important factor in suppressing the Mn dissolution and improving the kinetic properties of the material, thus resulting in excellent cycling stability.

4 Conclusions

Rheological phase reaction was used for synthesizing Mn-based spinel cathode. A certain amount of Co was doped to improve the cycling performance of the Mn-based spinel cathode. The result of XRD studies showed that as-prepared Co-doped $LiMn_2O_4$ had well-ordered cubic spinel structure. The result of SEM studies showed that the Co-doped $LiMn_2O_4$ had a perfect octahedral morphology. The results of charge–discharge tests indicated that rheological phase reaction and Co doping was effective for improving the cycling stability of Mn-based spinel cathode. All above results indicated that the rheological phase reaction method was an effective method to synthesize Co-doped $LiMn_2O_4$ cathode materials with superior electrochemical performance for lithium secondary battery.

Acknowledgments This work has been supported by the Natural Science Foundation of Ningxia: NZ14272 and the project from Ningxia Normal University: ZD201405.

References

1. F. Cheng, J. Liang, Z. Tao, J. Chen, Functional materials for rechargeable batteries. Adv. Mater. **23**, 1695–1715 (2011)

2. R. Pitchai, V. Thavasi, S.G. Mhaisalkar, S. Ramakrishna, Nanostructured cathode materials: a key for better performance in Li-ion batteries. J. Mater. Chem. **21**, 11040–11051 (2011)
3. L. Xiong, Y. Xu, C. Zhang, J. Li, Electrochemical properties of tetravalent Ti-doped spinel $LiMn_2O_4$. J. Solid State Electrochem. **15**, 1263–1269 (2011)
4. L.X. Zhang, Y.Z. Wang, H.F. Jiu, Y.L. Wang, Y.X. Sun, Z. Li, Controllable synthesis of Co-doped spinel $LiMn_2O_4$ nanotubes as cathodes for Li-ion batteries. Electron. Mater. Lett. **10**, 439–444 (2014)
5. W.H. Ryu, J.Y. Eom, R.Z. Yin, D.W. Han, W.K. Kim, H.S. Kwon, Synergistic effects of various morphologies and Al doping of spinel $LiMn_2O_4$ nanostructures on the electrochemical performance of lithium-rechargeable batteries. J. Mater. Chem. **21**, 15337–15342 (2011)
6. H. Zhao, X. Liu, C. Cheng, Q. Li, Z. Zhang, Y. Wu, B. Chen, W. Xiong, Synthesis and electrochemical characterizations of spinel $LiMn_{1.94}MO_4$ (M = $Mn_{0.06}$, $Mg_{0.06}$, $Si_{0.06}$, ($Mg_{0.03}Si_{0.03}$)) compounds as cathode materials for lithium-ion batteries. J. Power Sources **282**, 118–128 (2015)
7. W. Wen, B. Ju, X. Wang, C. Wu, H. Shu, X. Yang, Effects of magnesium and fluorine co-doping on the structural and electrochemical performance of the spinel $LiMn_2O_4$ cathode materials. Electrochim. Acta **147**, 271–278 (2014)
8. H.J. Bang, V.S. Donepudi, J. Prakash, Preparation and characterization of partially substituted LiMyMn2-yO4 (M = Ni Co, Fe) spinel cathodes for Li-ion batteries. Electrochim. Acta **48**, 443–451 (2002)
9. S. Mandal, R.M. Rojas, J.M. Amarilla, P. Calle, N.V. Kosova, V.F. Annufrienko, J.M. Rojo, High temperature Co-doped $LiMn_2O_4$-based spinels. Structural, electrical, and electrochemical characterization. Chem. Mater. **14**, 1598–1605 (2002)
10. R. Li, M. Li, Enhancement of the electrochemical properties of $LiMn_2O_4$ by glycolic acid-assisted sol–gel method. Ionics **15**, 215–219 (2009)
11. Y.P. Fu, C.H. Lin, Y.H. Su, S.H. Wu, Electrochemical characteristic of $LiMn_{1.925}M_{0.075}O_4$ (M = Cr, Co) cathode materials synthesized by the microwave-induced combustion method. J. Power Sources **159**, 215–218 (2006)
12. H.L. Bai, X.Y. Zhou, C.C. Peng, J.M. Guo, Effect of β-cyclodextrin on electrochemical properties of $LiMn_2O_4$ synthesized by solid-state combustion synthesis. Adv. Mater. Res. **785–786**, 797–802 (2013)
13. Q. Jiang, Synthesis and characterization of spinel $LiMn_2O_4$ prepared by the cyclohexanone hydrothermal method. Rsc Adv **3**, 12088–12090 (2013)
14. J.P. Silva, S.R. Biaggio, N. Bocchi, R.C. Rocha-Filho, Practical microwave-assisted solid-state synthesis of the spinel $LiMn_2O_4$. Solid State Ion **268**, 42–47 (2014)
15. C. Wang, X. Ma, J. Cheng, X. Cao, J. Sun, Y. Zhou, Synthesis of $LiNi_{0.9}Co_{0.1}O_2$ cathode material for lithium secondary battery by a novel route. Mater. Lett. **61**, 556–560 (2007)
16. B.S. Liu, Z.B. Wang, Y. Zhang, F.D. Yu, Y. Xue, K. Ke, F.F. Li, Preparation of submicrocrystal $LiMn_2O_4$ used Mn_3O_4 as precursor and its electrochemical performance for lithium ion battery. J. Alloys Compd. **622**, 902–907 (2015)
17. M. Hirayama, H. Ido, K. Kim, W. Cho, K. Tamura, J. Mizuki, R. Kanno, Dynamic structural changes at $LiMn_2O_4$/electrolyte interface during lithium battery reaction. J. Am. Chem. Soc. **132**, 15268–15276 (2010)
18. G. Jin, H. Qiao, H. Xie, H. Wang, K. He, P. Liu, J. Chen, Y. Tang, S. Liu, C. Huang, Synthesis of single-crystalline octahedral $LiMn_2O_4$ as high performance cathode for Li-ion battery. Electrochim. Acta **150**, 1–7 (2014)